CONF-8209191--1

MEASUREMENTS OF THE MICROWAVE POWER IN THE WALL AT EBT-I/S

D. A. Rasmussen, D. B. Batchelor

Oak Ridge National Laboratory

and

O. E. Hankins

North Carolina State University

CONF-8209191

DE84 000199

DISCLAIMER

MEASUREMENTS OF THE MICROWAVE POWER IN THE WALL AT EBT-I/S*

D. A. Rasmussen, D. B. Batchelor

Oak Ridge National Laboratory

and

O. E. Hankins

North Carolina State University

An understanding of the microwave propagation and absorption in ELMO Bumpy Torus (EBT) is critical because the plasma production, the heating and the stabilization provided by the hot electron rings are dependent on these processes. A microwave power balance model has been proposed for EBT[1,2]. This paper will describe a series of simple experiments designed to test this model by comparing its predictions and assumptions to both calorimetric and broad beam antenna measurements of the microwave power at the wall in EBT-I/S.

The theoretical picture of microwave propogation and absorption is one of weakly damped waves making many transits across the device with wall reflections and repeated ordinary/extraordinary mode conversions, playing an important part in the final energy deposition. A simple power balance model has been developed which treats the microwave sources, sinks and conversion processes in a globally averaged way. In the model the plasma is divided into three regions: (I) the low magnetic field side of cutoff external to the hot electron rings, (II) the low field side of cutoff internal to the rings, and (III) the high

*Research sponsored by the office of Fusion Energy, U. S. Department of Energy, under contract W-7405-eng-26 with the Union Carbide Corporation.

field side of cutoff (see Fig. 1). Energy balance equations are written for the sources, (injection, mode conversion, and tunneling) for each mode, in each region. Since a typical ray makes several reflections from cavity wall surfaces before being absorbed, additional simplifying assumptions are made that, after the first pass absorption, the wave fields are an isotropic, incoherent superposition of plane waves and that the energy density of each mode is uniform in a given region.

In the model, the energy balance equations are solved for the microwave energy density in each of the three regions defined above and also for the percentage of power absorbed in the three plasma components ring, core, and surface. The microwave power flux on the cavity wall is obtained from the energy density in region I. The level of power incident on the wall is an indication of the global absorption rate by the plasma. A high absorption rate decreases the amount of power reflecting around in the cavity (stored microwave energy) and therefore, reduces the microwave power flux on the wall.

The microwave power flux was measured with calorimeters. A sketch of one of them is shown in Fig. 2. Essentially all of the microwave power incident on the aperture of the calorimeter is absorbed by the circulating water load. Refections were measured to be less than 1%. The temperature rise of the water is therefore a measure of the microwave intensity at the cavity wall. A 25-watt cw 18-GHz source coupled directly to the calorimeter was used for calibration. Measurements were made simultaneously on two different EBT cavities N4

and S5 (see Fig. 3). Both cavities can be fed independently with 18-GHz power but cavity S5 does not have a feed for the 28 GHz. This feature was useful for the intercavity coupling experiments described later.

Figure 4 shows the measured power from each cavity as a function of total 18-GHz power into the EBT-I device at fixed pressure. Also plotted in the figure is the power balance model prediction - where an offset has been added to adjust for calorimeter heating due to conduction through the copper elbow from the EBT device. The calorimeters respond linearly implying that the microwave absorption coefficient is not a function of power and that the heat loss between the calorimeter and the temperature sensor is small. Also shown in the figure is the ratio of power at the calorimeter aperture (W_{cal}) to the heating power coupled to its cavity (W_{in}) after corrections are made for the calorimeter efficiencies and the waveguide distribution system losses. The ratios compare quite well with the model prediction of $P_{cal}/P_{in} \sim .10$, falling within the error bars of the model and the experimental accuracy. An attempt was made to understand the different ratios measured in S5 and N4 by swapping them from one cavity to the other. Table 1 shows measurements, under the same plasma conditions, made before (underlined) and after the swap. These results do not allow any conclusions to be drawn about whether the cavity location or the particular calorimeter is responsible for the discrepancy in ratios. Measurements at 28 GHz in EBT-S were also in good agreement with the model prediction of $P_{cal}/P_{in} \sim .12$.

Shown in Fig. 5 is the measured power received by the calorimeter as a function of torus fill pressure. In a qualitative manner the model predicts this behavior because at higher pressures the ring absorption disappears leaving a lower global plasma absorption.

Intercavity coupling experiments were performed to allow further testing of the model. By turning off the power to one or more of the cavities, the power coupled though the mirror throats can be determined. The cavities are individually fed at 18 GHz so that measurements can be made with various feed configurations. The feed to the central cavity containing the calorimeter can be turned off while the adjacent (and the other 21) cavities are left on, or the adjacent cavities can be turned off while the central cavity is fed. In addition to the mirror throats, intercavity coupling can also occur through the vacuum/28 GHz distribution manifold. For this reason, cavity S5 was chosen for the measurements because it does not have a manifold connection and therefore, all the coupling occurs through the mirror throats. The EBT-I model predictions for these feed configurations (normalized to the case where all the cavities are fed) are 37% and 70%, respectively. The results for these two configurations were obtained assuming the plasma parameters do not change, that is no attempt was made to self-consistently correct the change in absorption due to the different plasma conditions that result when power to a cavity is cutoff. However, hard x-ray measurements[3] on an unfed cavity indicate that the hot electron density is reduced about a factor of 10. Other model sensitive plasma parameters (surface plasma density and core density and temperature) are not observed to change more than about 10%[4]. Assuming that the ring absorption is zero in the unfed cavities, and that all other plasma parameters are unchanged, the model predicts 46% and 73% for the two feed configurations. Fig. 6 shows the EBT-I experimental results, in absolute value and as a percentage of the all fed configuration, for the calorimeter on cavity S5 at several different fill-pressure levels from 0.4-1.4 x 10^{-5} Torr.

The agreement while not outstanding is still quite good with both the model and experiments indicating that a large fraction of the microwave power is coupled between cavities. Measurements in EBT-S showed a coupling of approximately 31% to an unfed cavity while the model predicts a coupling of 36% assuming no change in ring absorption and 47% assuming that the ring absorption is zero in the unfed cavity. The good agreement, between the model and these intercavity coupling results, lends credence to the model assumption of weakly damped ordinary mode waves which are free to travel from cavity to cavity.

A set of measurements were also made with a fundamental mode waveguide stub receiver placed at the edge of the cavity. The stub was mounted in a vacuum ball joint which allowed it to be swept 5 cm's across the cavity port opening. This stub has a broad antenna pattern, which does not vary significantly over the $\pm 9^{o}$ sweep angle. Measurements made on a fed cavity at 18 GHz show considerable spatial variation (Fig. 7a) indicating some type of cavity mode structure. The details of the spatial structure are very plasma parameter dependent. Slight changes ($\lesssim 5\%$) in the operating pressure and/or microwave power level result in an entirely different spatial pattern. The results are, however, extremely reproducible. Measurements made 30 minutes apart at the same plasma parameters can be reproduced with only slight differences. Fig. 7b shows the result when the cavity is unfed and only the power coupled through the throats is measured. The lack of spatial structure seen in 7b supports the model assumption that multiple wall reflections result in an isotropic power density. 90^{o} rotations of the waveguide stub in the feedthrough allowed measurements of both the O-mode and X-mode polarizations. For the unfed configuration the

measured power is essentially independent of polarization. Because very little of the X-mode polarization can propagate through the mirror throats (it is nearly 100% absorbed at the fundamental resonance) mode conversion upon reflection must be a strong effect. Again this verifies the model assumption that mode conversion upon reflection is one of the dominate processes in the power balance.

In conclusion, both calorimetric and waveguide measurements of the microwave power at the wall in EBT show reasonable qualitative and quantitative agreement with the power balance model predictions of the global absorption rate. In addition, the assumptions of weakly damped waves and strong ordinary/extraordinary mode conversions upon wall reflection are verified by the measurements.

1. D. B. Batchelor, R. C. Goldfinger, Nucl. Fusion 20 403(1980).
2. D. B. Batchelor, Nucl. Fusion 21 1651(1981).
3. D. L. Hillis, Private communication.
4. R. K. Richards, Private communication.

Table 1. Measured 18-GHz power in watts for calorimeters A and B when alternately placed on cavities N4 and S5

	S5	N4
A	49	80
B	114	104

Fig. 1. Three region power balance model showing the location of each region and the microwave cutoff and resonant surfaces. Also shown are the regions of core, surface and annulus plasma.

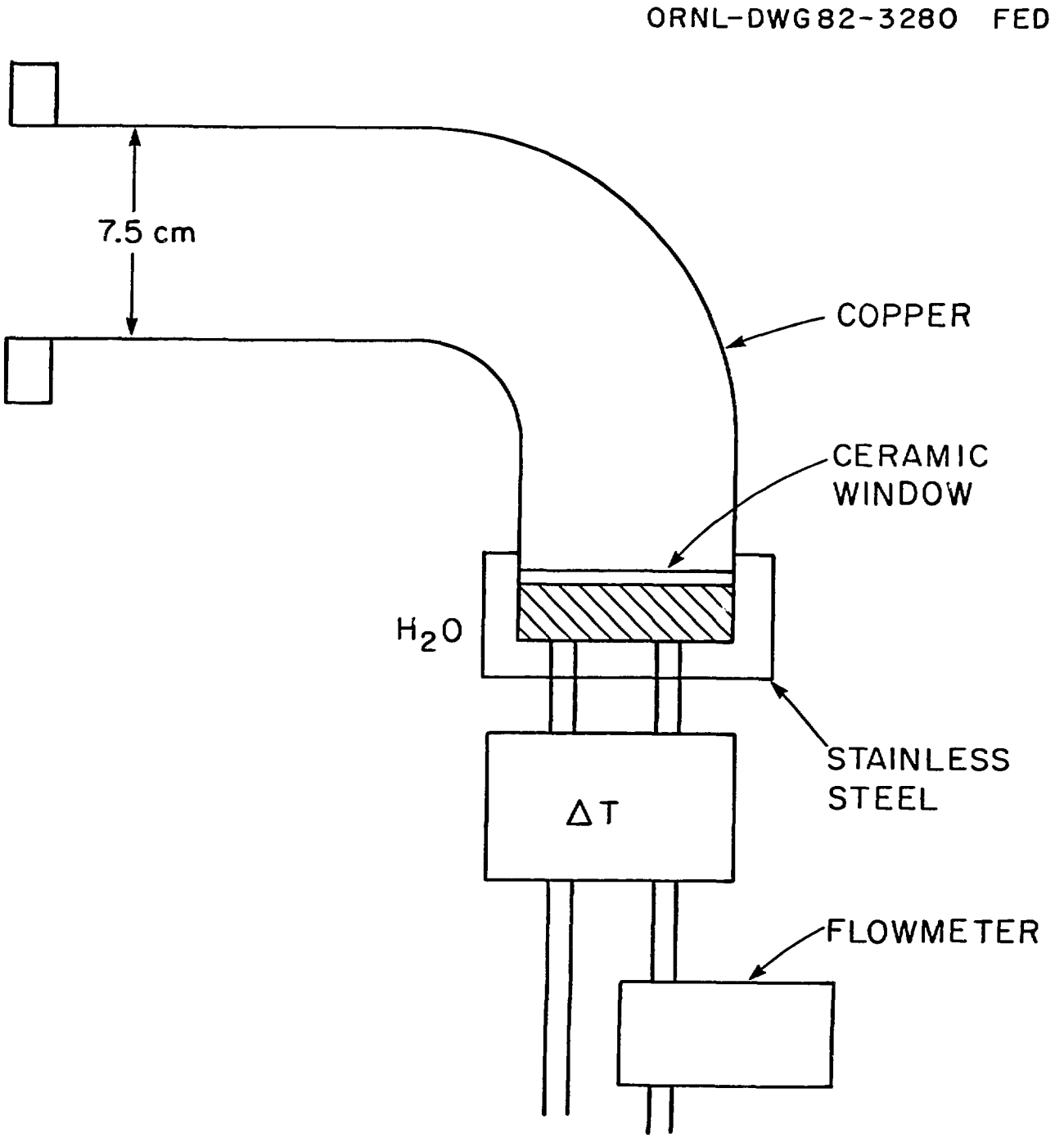

Fig. 2. Microwave Calorimeter. Microwaves are absorbed by the circulating water behind the ceramic window. Absorbed power is calculated from the measured temperature rise and the flow rate. The elbow prevents coating of the window by aluminum sputtered from the vacuum chamber walls.

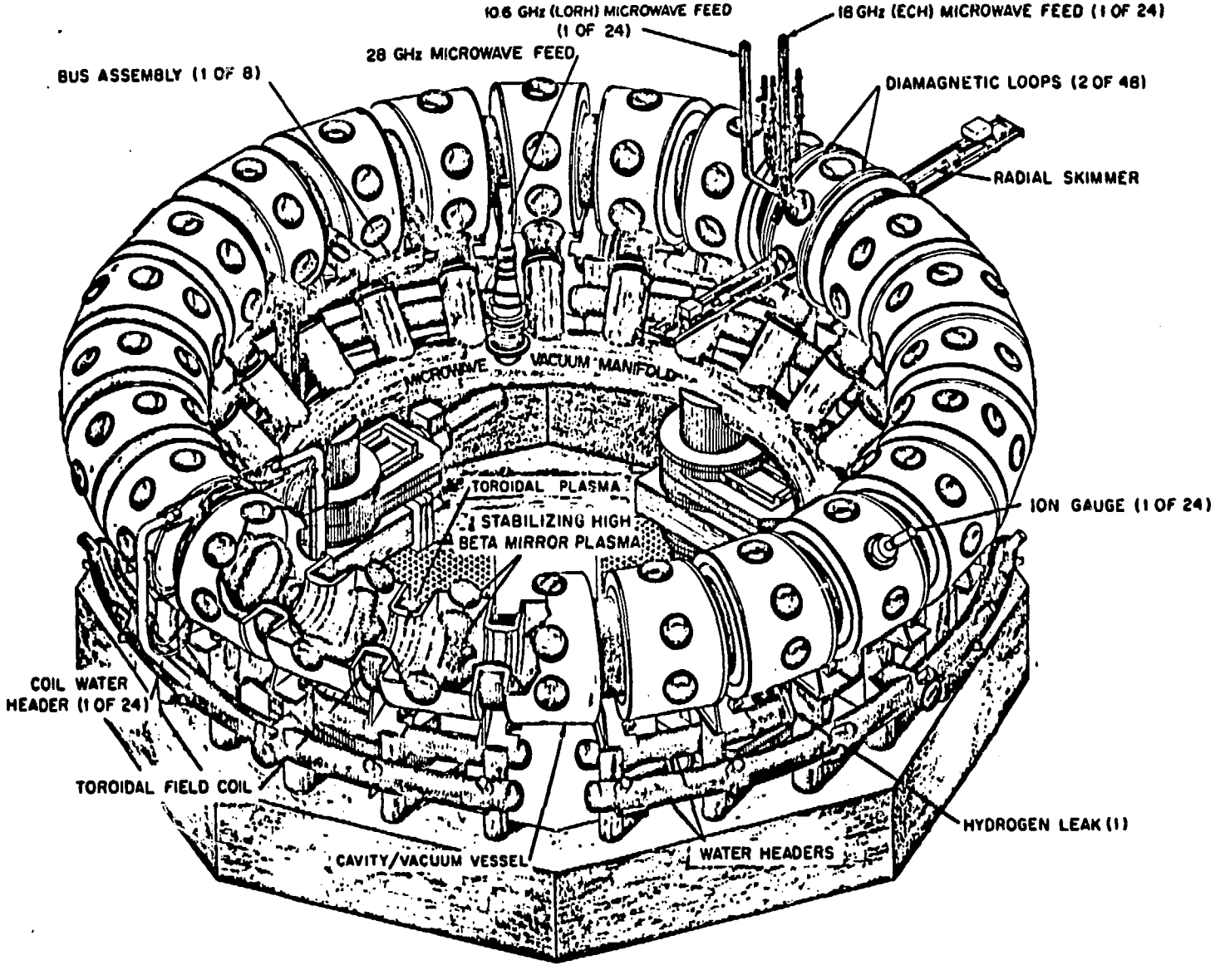

Elmo Bumpy Torus.

Fig. 3. Elmo Bumpy Torus device showing 1 of 24 of the 18 GHz microwave feeds and the microwave/vacuum manifold used to feed the 28 GHz power.

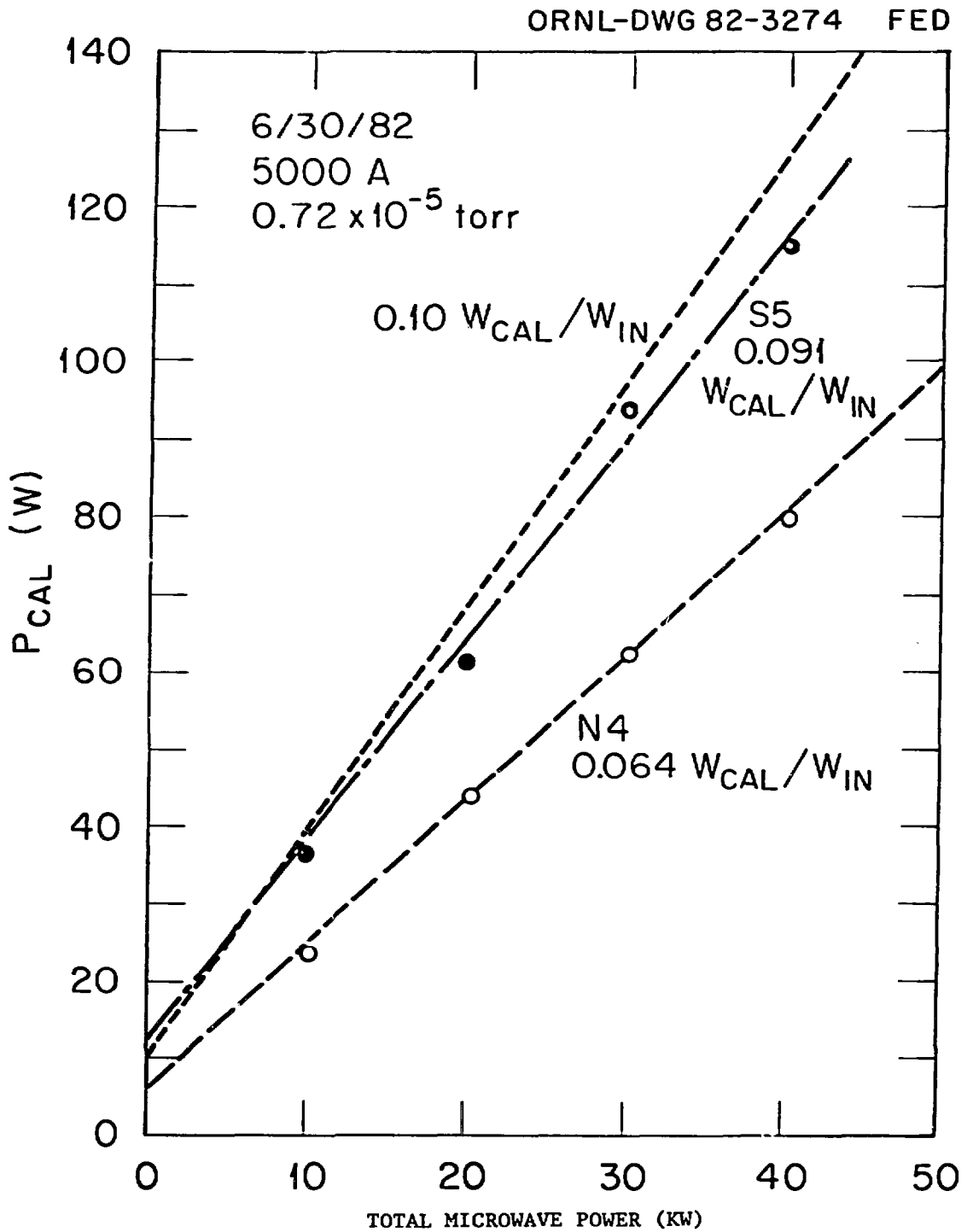

Fig. 4. Received power as a function of total power input in EBT-I for calorimeters on cavities S5 and N4. The short dash curve (slope 0.10) represents the power balance model prediction.

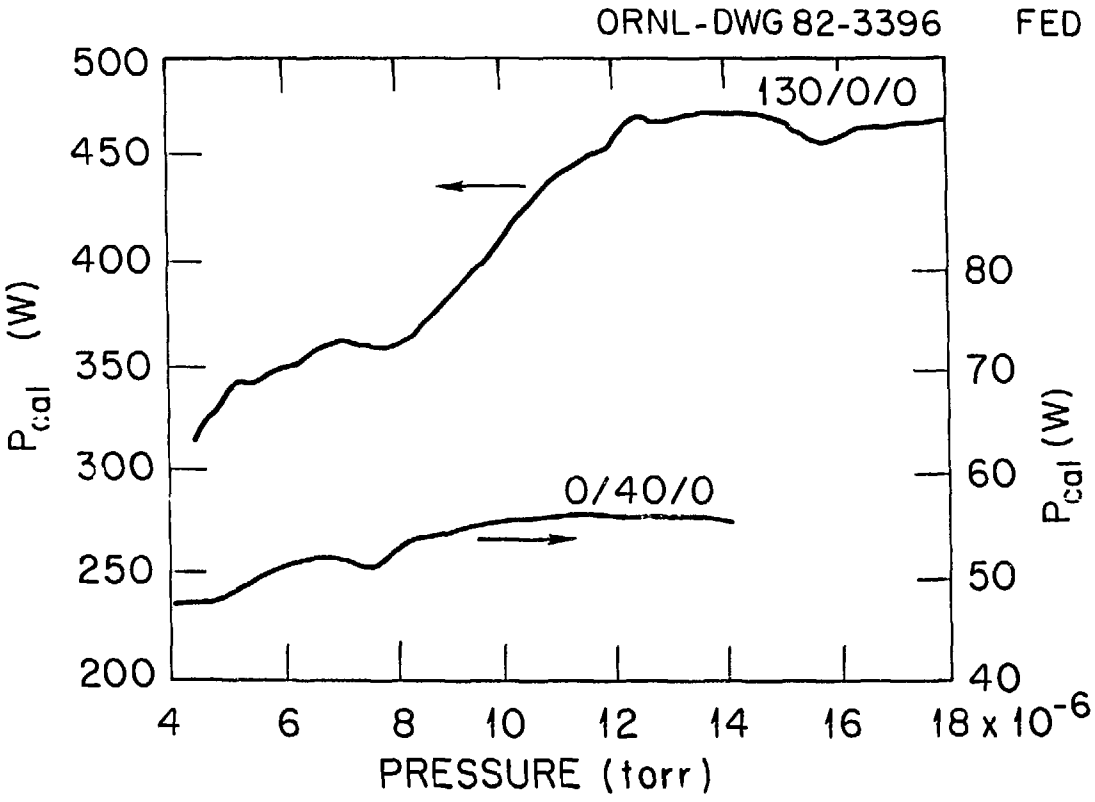

Fig. 5. Calorimeter received power as a function of pressure with the microwave power level at each frequency given as 28 GHz/18 GHz/10.6 GHz. The trend toward higher calorimeter power with increasing pressure is consistent with the power balance model predictions.

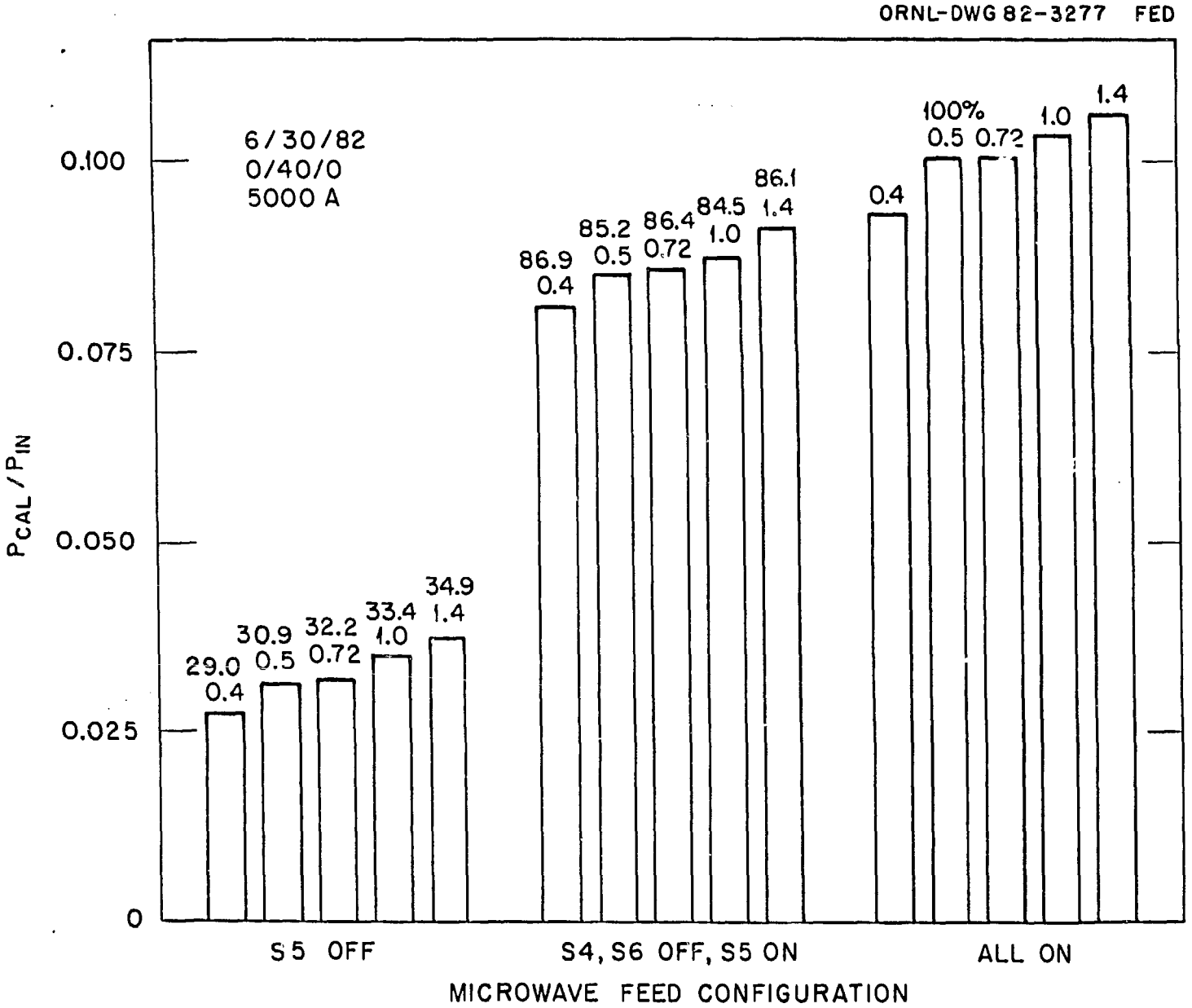

Fig. 6. Intercavity coupling results for a calorimeter on cavity S5 at various operating pressures from 0.4×10^{-5} to 1.4×10^{-5} Torr. Bar graphs are labeled as a percentage of the all fed configuration at the corresponding pressure.

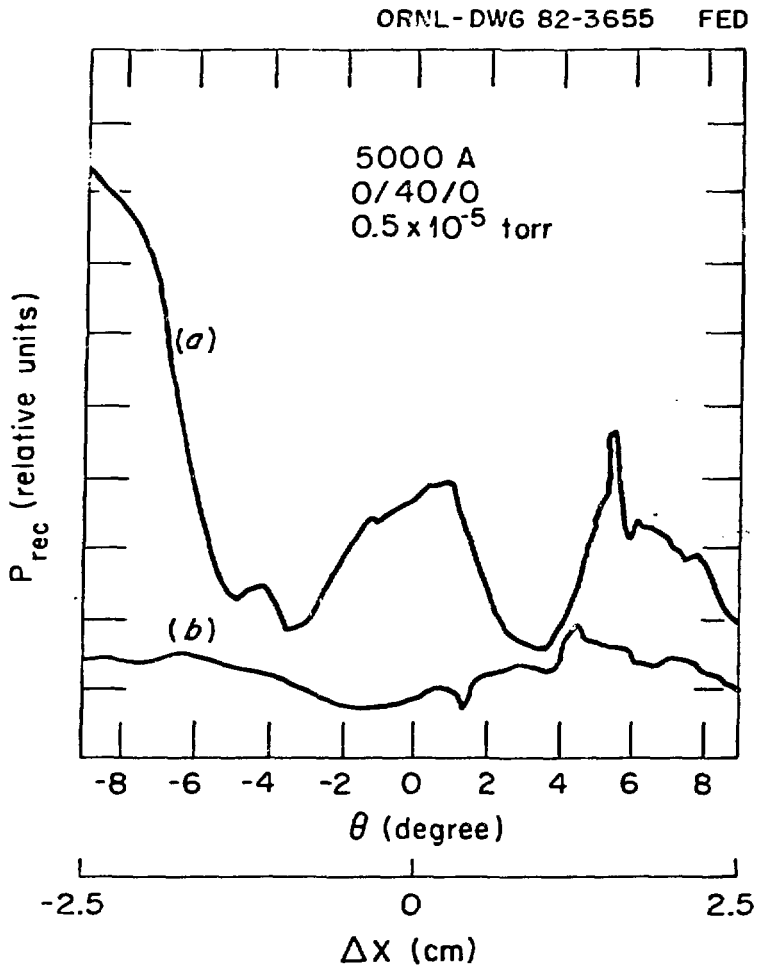

Fig. 7. Spatial variation of the microwave power density for a fed cavity (a) and an unfed cavity (b) at an operating pressure of 0.5×10^{-5} Torr.